PHYSICAL REVIEW B VOLUME 28, NUMBER 10 15 NOVEMBER 1983

High-temperature infrared-reflectivity study of the soft mode in $KTa_{1-x}Nb_xO_3$ for a Nb concentration $x=0.018$

D. Rytz
Institut de Physique Expérimentale, Ecole Polytechnique Fédérale de Lausanne (Swiss Federal Institute of Technology), CH-1015 Lausanne, Switzerland

M. D. Fontana
Laboratoire de Génie Physique, Université de Metz, F-57045 Metz, France

J. L. Servoin and F. Gervais
Centre de Recherches sur la Physique des Hautes Températures, Centre National de la Recherche Scientifique, F-45045 Orléans Cedex, France

(Received 13 December 1982; revised manuscript received 8 August 1983)

By performing infrared-reflectivity measurements on a $KTa_{0.982}Nb_{0.018}O_3$ crystal in the temperature range $300 \leq T \leq 1300$ K, an important deviation from the Curie-Weiss law is evidenced in the temperature dependence of the soft mode. A saturation regime can be inferred in the limit of infinite temperature. At very high temperature, the soft mode appears to be coupled with the immediately-higher-lying polar mode. The behavior of the soft mode can be interpreted in the framework of a shell model taking into account a strongly anisotropic nonlinear polarizability of the oxygen ion.

I. INTRODUCTION

The microscopic origin of ferroelectricity in ABO_3 compounds has been the subject of several recent investigations,[1-12] both theoretical and experimental. Based on the fact that ferroelectricity seems to be unusual in ABX_3 structures with $X=$F or Cl, it was realized that the oxygen ion should play a major role. In a qualitative picture, a strongly anisotropic electronic deformability is ascribed to the oxygen ion whose $2p$ electrons may move preferentially towards the empty d shells of the B transition-metal ion. This is the idea originally developed by Migoni, Bilz, and Bäuerle,[1] who introduced in their shell model an anisotropic nonlinear oxygen polarizability. This microscopic model correctly reproduces the second-order Raman spectra and the temperature dependence of the soft mode in $KTaO_3$ and $SrTiO_3$ in the temperature range $0<T<300$ K. Although the latter two substances remain paraelectric down to the lowest temperature at which they have been measured, it was felt that true ferroelectricity also was related to the invoked mechanism. The availability of this model and of its pseudo-one-dimensional simulation,[3] where the essential features are reproduced by a diatomic linear-chain treatment with a nonlinear polarizability of one sublattice, stimulated several developments in the field. It is worthwhile to note that the calculations have been extended to structurally completely different compounds such as PbS, PbSe, SnTe, and PbTe,[4] in which, with respect to a ferroelectric soft-mode description, the chalcogenide ion plays the pathological role of the oxygen. Furthermore, the model provides a description of both the incommensurate and the ferroelectric transitions of K_2SeO_4 (Ref. 5): In this case, the nonlinear polarizability is attributed to the SeO_4 units.

Experimental support to the model is provided by numerous investigations. The shift of the ferroelectric soft-mode frequency with oxygen vacancy concentration observed in $SrTiO_{3-x}$ (Ref. 6) has been quantitatively explained.[3] In "true" ferroelectrics, predictions of the model have been verified in $BaTiO_3$ (Ref. 7) (increase of the paraelectric-to-ferroelectric phase transition temperature induced by a strong magnetic field) and in $KNbO_3$ (Ref. 8) (splitting of the soft mode at the cubic-to-tetragonal ferroelectric transition). Most recently, a Mössbauer study of $LiTaO_3$ (Ref. 9) demonstrated a charge transfer from the neighboring oxygen ions to the central tantalum ion increasing nonlinearly with temperature, thus confirming directly the basic postulate of the model.

The present work is concerned with an interesting consequence of this model, which predicts an important deviation of the soft-mode frequency squared, Ω_s^2, from usual Curie-Weiss law, $\Omega_s^2 \sim A(T-T_c)$: At high temperature, Ω_s^2 tends to a limiting value of the frequency squared (the so-called "rigid-ion" value[2]), and thus a saturation of the hardening of the ferroelectric soft mode should be observed. Following a study of the low-temperature properties of the $KTa_{1-x}Nb_xO_3$ mixed-crystal system,[10] where the dielectric susceptibility behavior could be correctly analyzed within the Migoni-Bilz-Bäuerle model, we investigate here the high-temperature range from 300 to 1300 K (Ref. 11) with the aim to discuss the applicability of the model over a wide temperature range (i.e., from liquid-helium temperature up to the melting point). Furthermore, it appeared desirable to confirm in a true ABO_3 ferroelectric this very saturation effect previously observed in SbSI (Ref. 12) (with an anisotropic nonlinear polarizability

ascribed to the sulfur ion) and in the quantum paraelectric $SrTiO_3$.[13]

II. $KTa_{1-x}Nb_xO_3$ MIXED CRYSTALS

Historically the $KTa_{1-x}Nb_xO_3$ system has been the subject of several investigations aimed at testing its promising electro-optic properties.[14] In order to operate high-efficiency devices at room temperature, it appeared desirable to adjust the paraelectric-to-ferroelectric transition temperature just below 300 K. Knowing the ferroelectric phase diagram determined by Triebwasser[15] in the range $0.05 \leq x \leq 1.00$, one realizes that this condition requires $x \approx 0.35$. In the 1960s and early 1970s, numerous groups worked intensely on that system, but it appeared increasingly difficult to grow crystals of required quality and size,[14] and thus $KTa_{1-x}Nb_xO_3$ never reached the level of practical applicability. The system was rediscovered recently in the course of phase-transition studies dealing with the role played by impurities in the vicinity of such transitions. Several dopants (not only Nb, but also Li and Na) entering the $KTaO_3$ lattice in a substitutional position have been studied. Although "pure" $KTaO_3$ is a quantum paraelectric, the substitution of Ta by Nb (Ref. 16) or K by Na (Ref. 17) may render the system ferroelectric with very low transition temperatures. Most interestingly, as $k_B T_c$ is of the order of the zero-point energy, the influence of quantum fluctuations can thus be investigated in this case. The substitution of K by Li leads to a different class of phenomena[18] that needs further research for complete understanding.

More specifically, the phase diagram of the $KTa_{1-x}Nb_xO_3$ system[16] shows that, for $0.008 \leq x < 0.05$, a ferroelectric phase transition is observed at a transition temperature T_c that varies as $(x - x_c)^{1/2}$. The critical concentration $x_c = 0.008$ defines the quantum limit. For concentrations below this limit, no transition occurs at positive temperatures. This corresponds to the quantum paraelectric case, a case including pure $KTaO_3$ ($x = 0$). In our study we have chosen a $KTa_{1-x}Nb_xO_3$ crystal having a transition temperature of 28 K as determined from dielectric and ultrasonic resonance measurements using a conventional radio-frequency bridge technique. Figure 1 displays the peak of the static dielectric constant ϵ_0 and the step in the elastic compliance s_{11}^{-1} observed at $T_c = 28$ K. This T_c value corresponds to a concentration $x \simeq 0.018$ as obtained from the above-mentioned phase diagram.

Before starting with the actual infrared-reflectivity experiment (Sec. III) and describing the results (Sec. IV) that will be discussed in Sec. V, let us briefly mention previous phonon data obtained in $KTaO_3$ and in $KTa_{1-x}Nb_xO_3$ by various techniques: Infrared reflectivity ($KTaO_3$ and $K_{1-x}Na_xTaO_3$, Refs. 19–21), neutron scattering ($KTaO_3$, Ref. 22; $KTa_{1-x}Nb_xO_3$, Ref. 23), and Raman scattering ($KTaO_3$, Refs. 24 and 25; $KTa_{1-x}Nb_xO_3$, Refs. 26–29). It appears that infrared reflectivity is extremely well suited for polar-mode spectroscopy[30] and, in particular, soft-mode spectroscopy, as will be described in the following section.

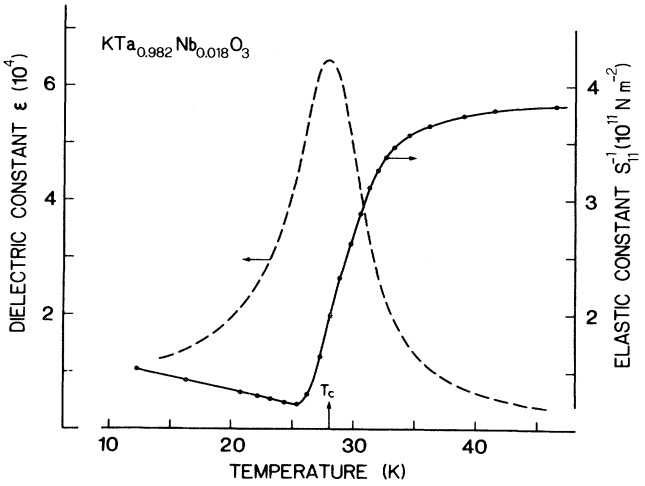

FIG. 1. Behavior of the dielectric and elastic constants near the ferroelectric phase transition at $T_c = 28$ K in $KTa_{0.982}Nb_{0.018}O_3$.

III. EXPERIMENT AND DATA ANALYSIS

The sample employed for the infrared-reflectivity measurements described below was a rectangular shaped plate of $18 \times 9 \times 0.7$ mm^3 with faces cut parallel to a (100) plane. The original crystals were grown by a flux method described in Ref. 31. It should be pointed out that due to the growth method a concentration gradient of 0.002 mol/mm is present along the plate thickness thus leading to a distribution of T_c across the sample. In the temperature range of interest, however, this effect is not relevant because measurements are made far above T_c. Owing to the high value of the absorption coefficient (from ~ 5000 cm^{-1} near the highest LO-mode frequency up to $\sim 25\,000$ cm^{-1} in the soft-mode frequency range), the penetration depth of the infrared radiation remains small at infrared frequencies. In order to analyze true bulk properties we have carefully annealed the sample for some hours at high temperature to regenerate the surface partially altered by polishing.

Reflection spectra on such single crystals have been performed by scanning interferometry over a wide wavenumber range (10–5000 cm^{-1}). The spectrometer (Bruker IFS 113) and its equipment for measurements up to high temperatures have already been described in detail in Ref. 32. Figure 2 shows the temperature dependence of infrared reflectivity from room temperature up to 1305 K. The ir spectrum performed at room temperature is in good agreement with data previously obtained on pure $KTaO_3$.[19–21] This is an indication that a small amount of niobium does not significantly alter the dynamical properties with respect to pure $KTaO_3$ in this temperature range. The static dielectric constant ϵ_0, which can be deduced from the low-frequency reflection level through the relation

$$\epsilon_0 = [(1+\sqrt{R_0})/(1-\sqrt{R_0})]^2 \quad (1)$$

is in good agreement with the experimental values mea-

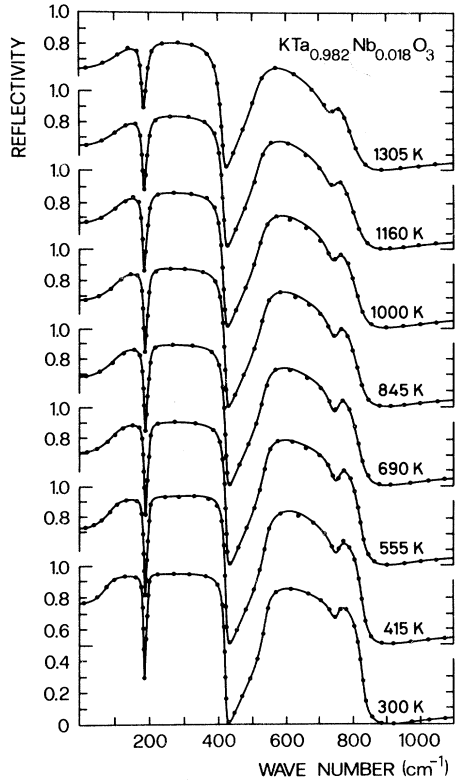

FIG. 2. Infrared-reflection spectra as a function of temperature. Curves are best fits to reflectivity data obtained with Eq. (2).

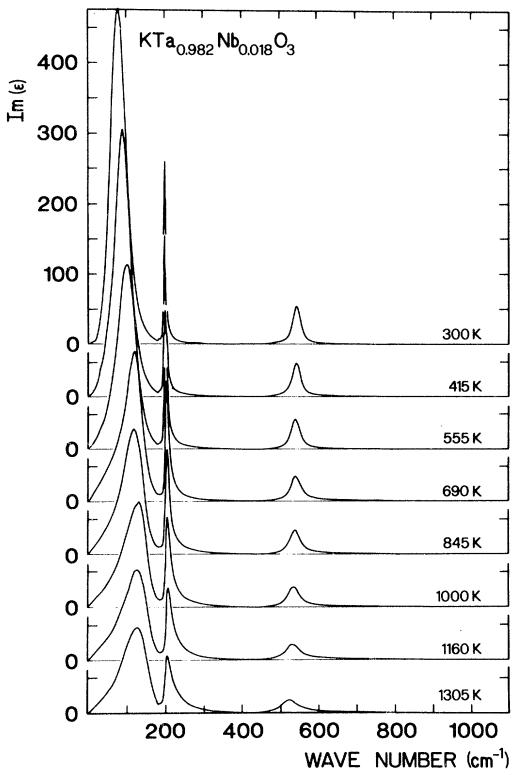

FIG. 3. Temperature dependence of the imaginary part of the dielectric function as obtained from a Kramers-Kronig analysis.

sured in the (1—100)-kHz range (see Fig. 1 and Refs. 33 and 34).

The evolution observed for the low-frequency reflection level with increasing temperature can be easily related, through the Lyddane-Sachs-Teller relation to the temperature dependence of the soft-mode frequency and constitutes therefore an accurate measurement of this quantity. The hardening of the lowest-frequency TO phonon—the ferroelectric (FE) mode—upon heating is clearly evidenced in Fig. 3 which displays the evolution of TO-mode structure in the studied temperature range, as obtained from a Kramers-Kronig analysis of reflectivity data.

First attempts by Spitzer *et al.*[35] to fit infrared spectra of TiO_2, $BaTiO_3$, and $SrTiO_3$ with classical dispersion theory failed. Barker and Hopfield[36] then developed the coupled—TO-mode theory of infrared dispersion to palliate this weakness. The interaction between modes introduces line asymmetries which can be understood otherwise in terms of frequency-dependent damping functions. In ferroelectric perovskites, the soft TO mode and the next TO mode exhibit level-repulsion behavior, which is characteristic of coupling, but also allows the determination of the coupling constant in first approximation. This coupling appears through the beginning of oscillator-strength—transfer phenomenon between both modes (see Fig. 3).

Another way to fit such broad reflection band spectra is to use the factorized form of the dielectric function,

$$\epsilon(\omega)=\epsilon_\infty \prod_j \frac{\Omega_{j\mathrm{LO}}^2-\omega^2+i\omega\gamma_{j\mathrm{LO}}}{\Omega_{j\mathrm{TO}}^2-\omega^2+i\omega\gamma_{j\mathrm{TO}}}\ , \tag{2}$$

as first introduced by Berreman and Unterwald.[37] This dielectric-function model, where two adjustable parameters—frequency Ω_j and damping γ_j—are introduced for each TO and LO vibrational mode, has been found to yield excellent fits in $BaTiO_3$,[38,39] $SrTiO_3$,[13] $KNbO_3$,[40] and $NaNbO_3$ (Ref. 41) without the need to invoke off-diagonal coupling terms in the phonon-response matrix. To illustrate this latter point of view, a comparison is drawn in Fig. 4 of best fits of classical and

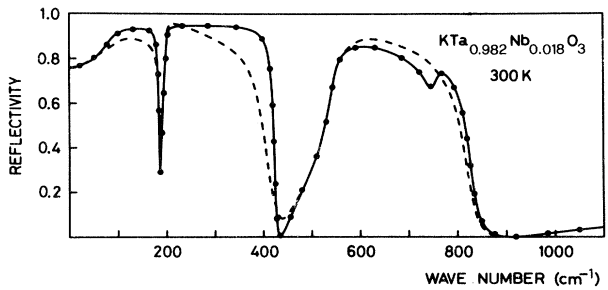

FIG. 4. Comparison between fits with the classical (dashed line) and the factorized forms of the dielectric function (solid line) to reflectivity data (closed circles).

factorized-form dielectric-function modes to the room-temperature infrared spectrum of $KTa_{0.982}Nb_{0.018}O_3$.

Examples of fits of Eq. (2) to experimental data in $KTa_{0.982}Nb_{0.018}O_3$ are shown in Fig. 2 and found to closely reproduce the reflection spectra. The parameters which yield the best fits to the data at room temperature and 1305 K are discussed below. Figure 5 displays an example of good agreement between the dielectric response function evaluated from a Kramers-Kronig analysis and the factorized form which yields the best fit to reflectivity data.

IV. RESULTS

A. Oscillator strengths

From the expression of the factorized form of the dielectric function, the oscillator strengths of the phonon polar oscillators can easily be deduced as a function of the TO-LO splittings through the relation

$$\Delta\epsilon_j=\frac{\epsilon_\infty}{\Omega_{j\,\mathrm{TO}}^2}\frac{\prod_k(\Omega_{k\,\mathrm{LO}}^2-\Omega_{j\,\mathrm{TO}}^2)}{\prod_{k\neq j}(\Omega_{k\,\mathrm{TO}}^2-\Omega_{j\,\mathrm{TO}}^2)}\ . \tag{3}$$

Their temperature dependence is displayed in Fig. 6. By comparison with experimental static dielectric constant and oscillator-strength values, it can be clearly seen that the soft-mode oscillator strength constitutes nearly all the contributions to static ϵ_0. Upon heating, an intensity transfer between the soft mode and the next TO mode takes place in the high-temperature range as one approaches the anticrossing region. This coupling phenomenon will be discussed below.

B. Frequencies

Figure 7 displays the temperature dependence of TO and LO frequencies as obtained by fitting the reflection spectra. Data obtained by other, different techniques[33,34] are also reported at temperatures below room temperature. As previously observed in $SrTiO_3$,[13] mode frequencies above 400 cm^{-1} present a smooth decrease with increasing temperature. This is a common behavior since the effects of lattice thermal expansion (which tends to lower the force constants) plus cubic anharmonic couplings contribute to the down shift of the phonon frequency upon heating.

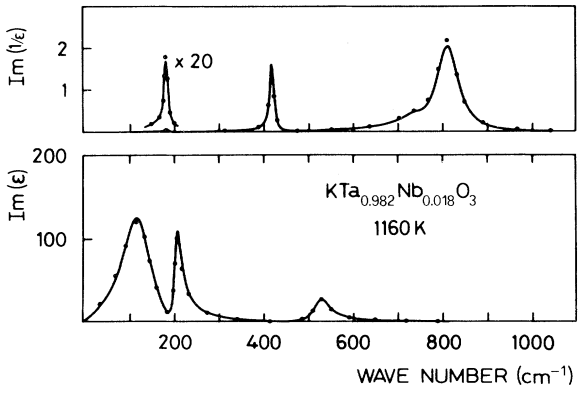

FIG. 5. Comparison between Kramers-Kronig analysis (solid circles) and the factorized form of the dielectric function (solid line).

Contrary to these modes, the second low-lying TO mode at 196 cm^{-1} increases with increasing temperature. The square of the frequency of the three lowest-energy modes is drawn as a function of temperature in Fig. 8, in parallel with similar results in $SrTiO_3$. The most striking feature of this figure is the important deviation for the soft-mode-frequency squared from the Curie-Weiss law. It should be emphasized that this deviation had been predicted in 1964 by Rupprecht and Bell[34] based on dielectric constant measurements (see Sec. V).

The second feature which clearly appears is the coupling between the two TO modes. Both modes have been decoupled with the aid of the usual formula,[42]

$$\Omega_\pm=\tfrac{1}{2}(\omega_1+\omega_2)\pm\tfrac{1}{2}[(\omega_1-\omega_2)^2+4W^2]^{1/2}\ , \tag{4}$$

where Ω_+ and Ω_- correspond to experimental coupled-mode frequencies. Approximating the uncoupled hard-mode frequency at 196 cm^{-1} to be roughly temperature independent, it is thus possible to have an idea of the minimum deviation from the linear law. Good fits to Ω_+

TABLE I. Parameters of the fits with $\gamma=1$ in Eq. (9) for various Nb concentrations in $KTa_{1-x}Nb_xO_3$.

Nb concentration x in $KTa_{1-x}Nb_xO_3$	T_0 (K)	ϵ_I	B (K)	Temperature range	Reference	Authors
0	2.8	39.32	59 890	3–323	34	Rupprecht and Bell
0	4	48	59 900	4–300	33	Wemple
0	11.8	48.3	55 200	4–300	33	Abel
0	13.1	47.5	54 500	4–300	33	Samara and Morosin
0	12.3	48.5	50 100	10–300	33	Lowndes and Rastogi
0	6.3	51.7	51 000	30–300	33	Lowndes and Rastogi
0	4	45	64 000	4–300	33	Ivanov *et al.*
0.006	20	59	50 000	8–300	10	Rytz *et al.*
0.008	30	72	45 000	14–300	10	Rytz *et al.*
0.012	32	60	46 000	24–300	10	Rytz *et al.*
0.018	38	52.2	48 200	300–1300		This work

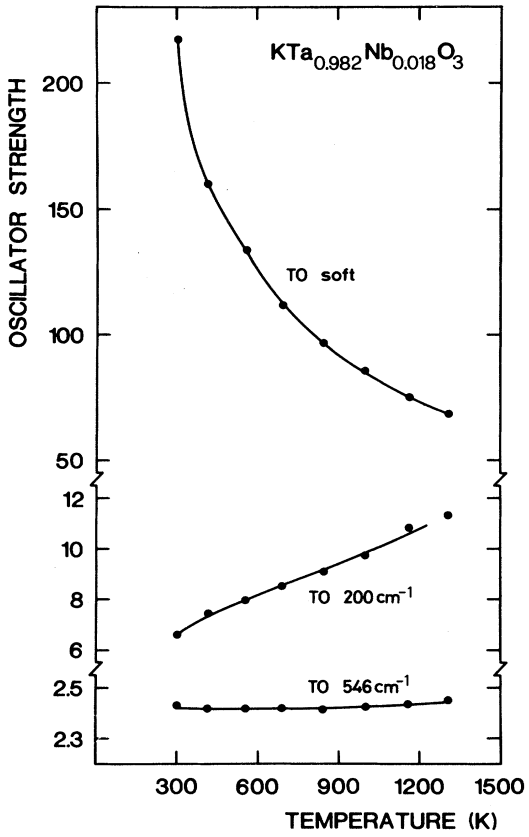

FIG. 6. Temperature dependence of TO oscillator strengths.

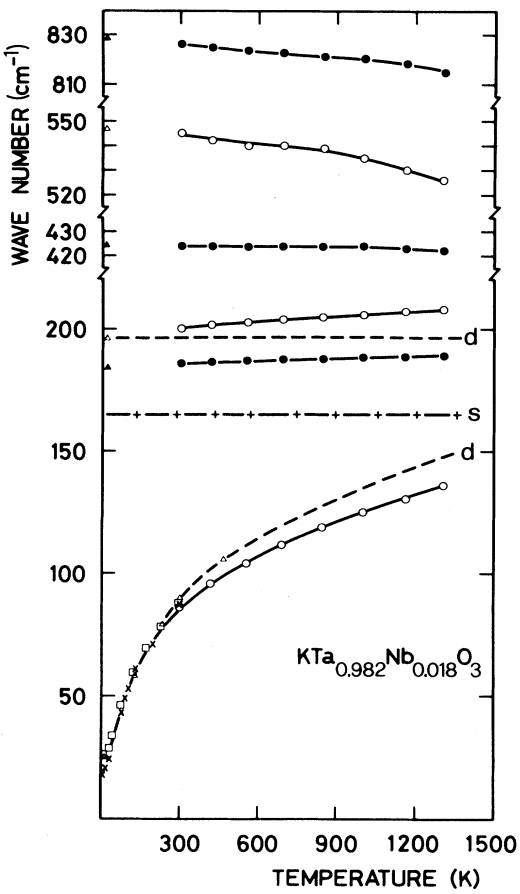

FIG. 7. Temperature dependence of optical frequencies. Open and closed circles are TO and LO modes, respectively. Other symbols are taken from Refs. 33 and 34. Dashed lines labeled *d* are decoupled frequencies [see Eq. (4)]. The dashed-crossed line labeled *s* is the infinite-temperature limit of the soft mode.

and Ω_- data can be obtained with a coupling constant $W=25$ cm^{-1}. The decoupled soft-mode frequency squared (Ω_{sd}^2) deduced from this fit is also plotted in Fig. 8 (subscript *d*). This deviation from the Curie-Weiss behavior is much more pronounced than in strontium titanate—as can be seen in those parallel figures—since at the highest temperature, Ω_{sd}^2 is $\sim$40% lower than the extrapolation from the linear regime which holds below 300 K, i.e., a result which is twice the value of the deviation in $SrTiO_3$. The coupling parameter thus obtained (25 cm^{-1}) is markedly higher than in $SrTiO_3$ (10 cm^{-1}). These values are weak with respect to the frequency of decoupled modes at the crossing.

C. Dampings

The temperature dependence of TO and LO dampings is displayed in Fig. 9. To study phonon lifetimes in $KTa_{1-x}Nb_xO_3$ we have used a model deduced from the imaginary part of the self-energy function which takes into account cubic additive anharmonic processes only, and which can be written in the form[43]

$$\gamma_j(T)=\gamma_j(0)[n(\tfrac{1}{2}\Omega_j(T))+\tfrac{1}{2}]\,, \tag{5}$$

where

$$n(\Omega)=[\exp(\hbar\Omega/k_BT)-1]^{-1} \tag{6}$$

is the mean number of phonons.

This model was shown to explain the temperature dependence of any damping constant in common oxide crystals which do not undergo structural phase transitions. All modes, however, can be satisfactorily described within this model as shown in Fig. 9. As might be expected, the model [Eq. (5)] does not agree so well when the mode shifts up considerably, as it is the case for the soft mode whose frequency increases from 86 to 136 cm^{-1}. The soft mode is weakly damped at low and intermediate temperatures and the ratio γ_s/Ω_s reaches 0.7 at 1300 K. The data obtained in the temperature range below 300 K, as obtained from electric-field-induced Raman scattering are in rather good agreement with our ir damping results. On the other hand, no damping transfer between the soft mode and the TO 196-cm^{-1} mode can be detected with certainty. This is not surprising since at the highest temperature both modes have not yet crossed each other.

Let us now discuss the feature which appears at all temperatures as a dip in the vicinity of 750 cm^{-1}. This particularity has already been mentioned by Perry and Torn-

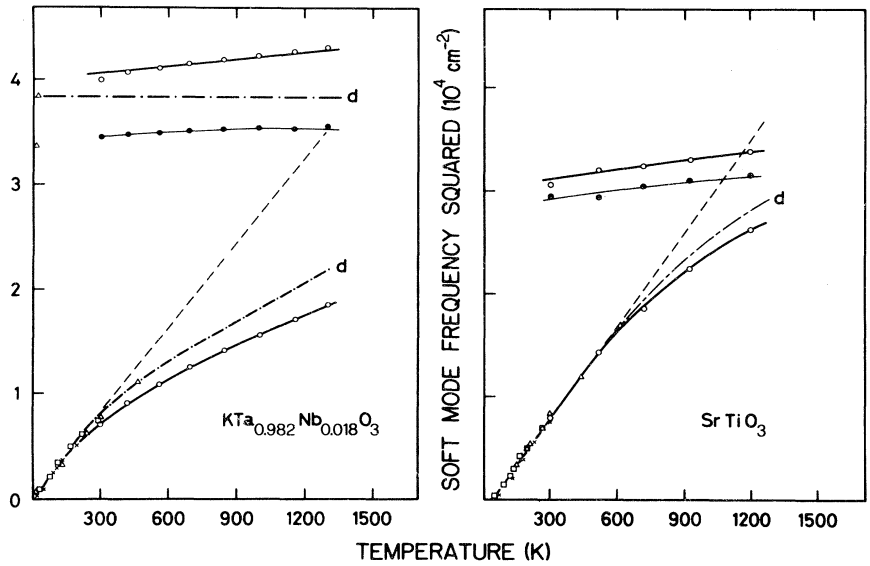

FIG. 8. Temperature dependence of the square of the frequencies. Dashed line is an extrapolation of the Curie-Weiss law. Same legend as for Fig. 7 holds for the other symbols. Comparison is made with the results obtained for $SrTiO_3$ in Ref. 13.

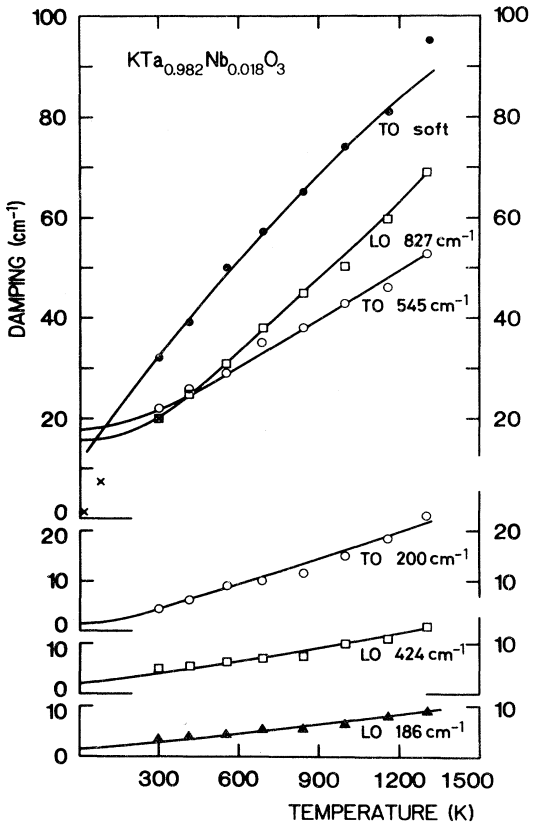

FIG. 9. Temperature dependence of dampings (closed circles). Solid lines are fits obtained with Eq. (5). Crosses correspond to data from Ref. 24.

berg.[21] In fact this kind of dip is usual in the high-frequency tail of reflection bands. It is customarily described as an additional oscillator and understood in terms of a multiphonon combination band. Another description, based on a phonon self-energy mechanism can be provided, as previously used to analyze such features in $LiTaO_3$ and $LiNbO_3$.[44,45] These dips can be unambiguously attributed to anharmonic effects. From Kramers-Kronig analysis it is possible to calculate the frequency-dependent imaginary part $\Gamma(\omega)$ of the phonon self-energy of the TO mode near 545 cm^{-1}; a peak which corresponds to the two-phonon density of states, and which becomes more and more intense with increasing temperature, appears near 700 cm^{-1} as displayed in Fig. 10. The dielectric-function model (Eq. 2) may be modified to take into account this two-phonon peak near 700 cm^{-1} (for more details see Refs. 44 and 45). This kind of treatment has been tested to provide good fits to the reflection data. But for simplicity, the reflection profiles obtained with the formalism of Eq. (2) only, plus two additional oscillators, have been displayed in Fig. 4.

V. DISCUSSION

A. Temperature dependence of the dielectric constant

It is now well established that in the incipient ferroelectrics $KTaO_3$ and $SrTiO_3$, and in ferroelectric $KTa_{1-x}Nb_xO_3$, the dielectric constant ϵ_0 does not follow a simple Curie-Weiss law of the form

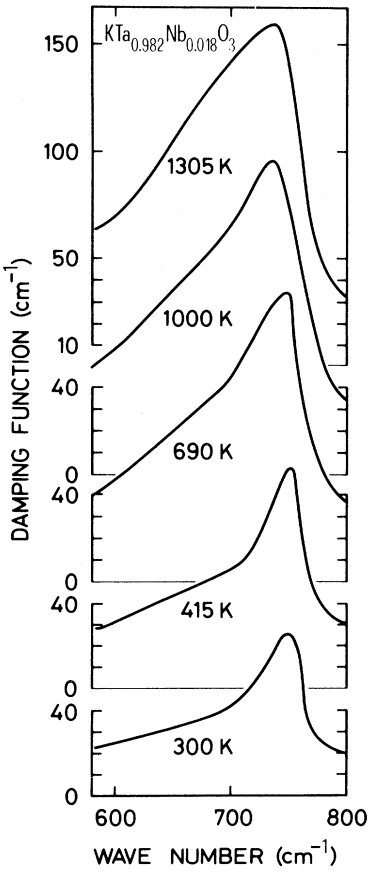

FIG. 10. Temperature and frequency dependence of the damping function of the TO mode at 545 cm^{-1} as deduced from Kramers-Kronig analysis.

$$\epsilon_0 = C(T - T_0)^{-1} , \tag{7}$$

where C and T_0 are the Curie constant and the Curie temperature, respectively. Many years ago Barrett[46] suggested another expression,

$$\epsilon = \epsilon_l + B[\tfrac{1}{2}T_1 \coth(T_1/2T) - T_0]^{-1} , \tag{8}$$

where T_1 defines the temperature below which the quantum effects are predominant. For the low-temperature regimes, however, in $SrTiO_3$ (Ref. 47) and in $KTa_{1-x}Nb_xO_3$ near the quantum limit,[10,27] a limited validity only could be ascribed to Eq. (8). More generally, the behavior of the dielectric constant can be described by the following expression[10,17]:

$$\epsilon_0 = \epsilon_l + B(T - T_0)^{-\gamma} , \tag{9}$$

where B is the Curie constant and ϵ_l represents the dielectric constant in the limit of infinite temperature. The critical exponent γ takes the values 2 and 1 at the quantum limit and in the classical regime ($100 < T < 300$ K), respectively. It should be noted that Eqs. (8) and (9) are equivalent in the classical regime ($T_1 \ll T$) for $\gamma = 1$.

With our experiments data are now available in a broad temperature range thus allowing an extensive test of the above-standing relations. As already mentioned in Sec. III, the static dielectric constant ϵ_0 is directly derived from the reflectivity level R_0 via

$$\epsilon_0 = [(1+\sqrt{R_0})/(1-\sqrt{R_0})]^2 .$$

At 300 K, our value ($\epsilon_0 = 235$) agrees indeed reasonably well with the measured[34] room-temperature value $\epsilon_0 = 240$. Moreover, this consideration is another way to say (see also Sec. IV A) that the dielectric constant is mainly due to infrared-active modes and that the contributions in the microwave region are negligible, in contrast to the case of ferroelectric $BaTiO_3$ (Ref. 38) and $KNbO_3$ (Ref. 40) for which an important discrepancy is observed between the values deduced from the Lyddane-Sachs-Teller relation and the direct measurements in a large temperature range around the transition.

Equation (9) with $\gamma = 1$ has been fitted to the measured temperature dependence of the dielectric response in the temperature range considered in our experiments ($300 < T < 1300$ K). Figure 11 clearly shows that the modified Curie-Weiss law of the form $\epsilon_0 = \epsilon_l + B(T - T_0)^{-1}$ is accurately obeyed in this region. Table I gives our parame-

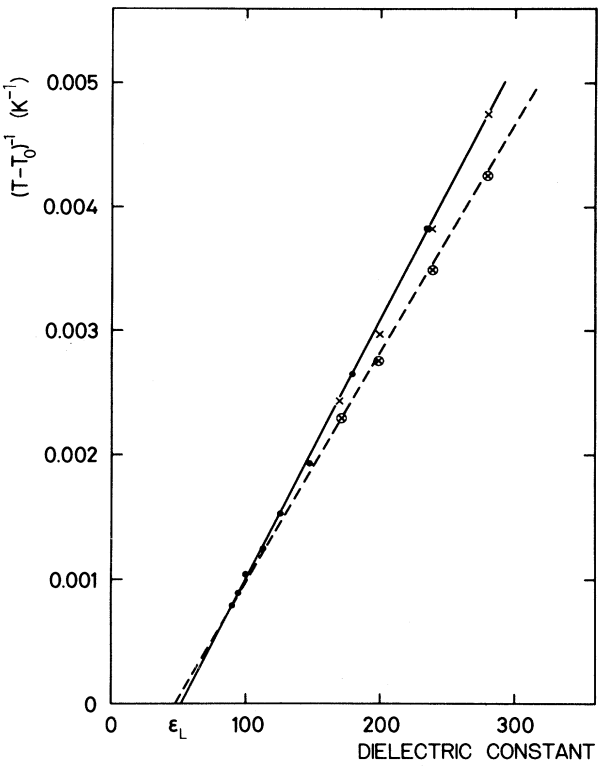

FIG. 11. Temperature dependence of the static dielectric constant of $KTa_{0.982}Nb_{0.018}O_3$. Solid line is a least-squares fit of Eq. (9) with $\gamma = 1$ to our data (solid circles). Crosses correspond to the measurements obtained in pure $KTaO_3$ by Samara and Morosin (Ref. 33). Dashed line represents their calculation extrapolated at high temperatures with their data points (circled crosses). Difference between the crosses and the circled crosses reflects the difference in T_0. Deviation from Curie-Weiss law appears as a nonzero value ϵ_l obtained at infinite temperature.

ter data and summarizes the results reported elsewhere in pure $KTaO_3$ and mixed-crystal $KTa_{1-x}Nb_xO_3$.

B. Temperature dependence of the soft-mode frequency

In order to understand the significance of the infinite-temperature limit ϵ_I of the dielectric constant and the origin of the saturation regime, Eq. (9) with $\gamma=1$ is expressed in terms of polar lattice vibrations using the Lyddane-Sachs-Teller relation

$$\epsilon_0=\epsilon_\infty \prod_j \frac{\Omega_{j\mathrm{LO}}^2}{\Omega_{j\mathrm{TO}}^2} , \tag{10}$$

where ϵ_∞ is the high-frequency dielectric constant. Our data clearly show that all LO and TO modes except the soft phonon mode are essentially temperature independent in the range 300—1300 K. Therefore, we denote A' the constant,

$$A'=\prod_j \Omega_{j\mathrm{LO}}^2 \Big/ \prod_j{}' \Omega_{j\mathrm{TO}}^2 , \tag{11}$$

where $\prod'$ is a product over all TO frequencies except the soft-mode frequency. The inverse of the soft-mode-frequency squared is therefore given by the relationship

$$\frac{1}{\Omega_s^2}=\frac{\epsilon_0}{\epsilon_\infty}\frac{1}{A'}=\frac{\epsilon_I}{\epsilon_\infty A'}+\frac{B}{(T-T_0)\epsilon_\infty A'}$$

or

$$\frac{1}{\Omega_s^2}=\frac{1}{\Omega_I^2}+\frac{A}{T-T_0} . \tag{12}$$

This expression is obviously different from the classical Curie-Weiss form: $\Omega_s^2=C(T-T_0)^{-1}$. It suggests that the soft-mode frequency does not increase indefinitely with temperature but approaches a limiting value at infinite temperature defined by the constant Ω_I. The adjustment of Eq. (12) to the experimental data yields the following values of parameters for $KTa_{1-x}Nb_xO_3$: $1/\Omega_I^2=0.37\times10^{-4}$ cm^2 ($\Omega_I=164$ cm^{-1}), $A=0.0263$ K cm^{-2}, and $T_0=38$ K. The law described by Eq. (12) is accurately satisfied in the range 300—1300 K, and the saturation value is found at 164 cm^{-1}. No direct calculations of these parameter values have been previously reported. Nevertheless, from dielectric constant data, Ω_I was estimated at 272 cm^{-1} by Rupprecht and Bell.[34] The large discrepancy arises because in their approximation they assumed that the soft-mode oscillator strength is temperature independent, while our measurements show that its value at 1300 K is a factor of 3 smaller than at 300 K.

This simple treatment resulting in Eq. (12) assumes that Eq. (9) is obeyed in the infinite-temperature limit, whereas its validity is experimentally shown to hold within less than 1 order of magnitude in Fig. 11. On the other hand, a deviation of ϵ_0 from the Curie-Weiss law is expected at very high temperature even if Ω_s still follows a Curie-Weiss behavior. This is due to the fact that the soft-mode contribution to ϵ_0 will become comparable to the contribution of the other modes, whereas $\Delta\epsilon_s\simeq\epsilon_0$ in the temperature interval between T_c and 1000 K (see Sec. IV A and Fig. 6). Nevertheless, irrespective of the above considerations, our direct measurements of the temperature dependence of the soft-mode frequency show a deviation from Curie-Weiss law above room temperature, even after decoupling the soft mode from the higher-lying TO mode (Fig. 8).

In order to discuss the origin of the temperature dependence of the soft mode and its saturation in the high-temperature limit, we consider the shell model originally used by Migoni *et al.*[1] for describing the dynamical properties of pure $KTaO_3$ from 0 to 300 K. This model, based on the quasiharmonic approximation, leads to a self-consistent calculation of the soft-mode-frequency squared Ω_s^2 under the assumption of an anisotropic nonlinear intraionic polarizability of the oxygen ion. We denote the core-shell force constants in the directions of neighboring K and (Ta,Nb) ions by k_{OA} and k_{OB}, respectively. The k_{OB} constant includes a harmonic k_2 term and an anharmonic fourth-order k_4 contribution,

$$k_{OB}(T)=k_2+\tfrac{1}{2}k_4\langle W^2\rangle_T , \tag{13}$$

where $\langle W^2\rangle_T$ is the self-consistent thermal average over the squared shell displacement at temperature T given by the relation

$$\langle W^2\rangle_T=\frac{\hbar}{2Nm_{\mathrm{O}}}\sum_{\lambda=1}^{N}\left|\frac{f_\alpha^2(\mathrm{O}_\alpha\,|\,\lambda)}{\Omega_\lambda}\right|\coth\left[\frac{\hbar\Omega_\lambda}{2k_BT}\right] , \tag{14}$$

where the f_α's are shell eigenvectors, $\lambda(q,j)$, and O_α denotes the oxygen (of mass m_0) whose neighboring (Ta,Nb) ions are located in α direction (x, y, or z). In this case, the temperature dependence of the soft-mode-frequency squared is given by

$$\Omega_s^2=\omega_0^2+\tfrac{1}{2}k_4\frac{f_0^2}{m_{\mathrm{O}}}\langle W^2\rangle_T , \tag{15}$$

where ω_0 and f_0 are the imaginary frequency and the shell eigenvector for the soft mode in the harmonic approximation, respectively. The large amplitude of the soft motion and the strong hybridization of the oxygen p states with the d states of the metal ion (Ta,Nb) enhance dynamically the intraionic oxygen polarizability along the $\langle 100\rangle$ axes, which is thought to be responsible for the instability occurring in the harmonic approximation. The crystal is stabilized only through the fourth-order coupling term via a renormalization of the soft-mode frequency. The other lattice modes are not affected by a change in the k_{OB} force constant. In comparison with the true anharmonic k_4 term, the thermal expansion is found to show an opposite but small effect on Ω_s^2. A similar result was obtained by Samara and Morosin[33] for $\epsilon_0(T)$ in pure $KTaO_3$.

At high temperature, where $\coth x\approx 1/x$, Eqs. (14) and (15) can be rewritten in approximate forms as

$$\langle W^2\rangle_T\sim\frac{k_B}{Nm_{\mathrm{O}}}T\sum_{\lambda=1}^{N}\frac{f_\alpha^2(\mathrm{O}_\alpha\,|\,\lambda)}{\Omega_\lambda^2} \tag{16}$$

and

$$\Omega_s^2=\omega_0^2+rT\ , \tag{17}$$

where

$$r=\frac{1}{2}\frac{k_B k_4}{Nm_O^2}f_0^2\sum_{\lambda=1}^{N}\frac{f_\alpha^2(O_\alpha\,|\,\lambda)}{\Omega_\lambda^2}\ . \tag{18}$$

The quantity r decreases with temperature owing to the variation of $f_\alpha(O_\alpha\,|\,\lambda)$. Therefore Ω_s^2 does not depend linearly on T.

The model allows an interpretation of the deviation from the linear (i.e., Curie-Weiss) law and predicts the saturation in the infinite-temperature limit. Figure 12 illustrates the relationship between the temperature dependence of $\langle W^2\rangle_T$ or Ω_s^2 and the f^2/Ω_λ contributions for the two lowest modes at $q=0$.

In fact, at relatively low temperatures (300 K) the contribution of the soft optic branch in the calculation of $\langle W^2\rangle_T$ [Eqs. (14) or (16)] is dominant since it is the very mode which is strongly temperature dependent. The corresponding eigenvectors are much larger than those of the other branches. With increasing temperature the anharmonic interactions between the soft mode and the other normal modes of vibration increase and so do $\langle W^2\rangle_T$, $k_{OB}(T)$, and Ω_s^2. There is a beginning of eigenvector transfer between the soft motion, which corresponds to a vibration of the (Ta,Nb) ion relative to the oxygen octahedron, and the next TO vibration, which consists of a displacement of K ions against TaO_6.[48] At 300 K, the oxygen-shell eigenvector of the second mode indeed represents $\frac{1}{4}$ in relative weight as compared to the first mode, but nearly $\frac{1}{2}$ at 1300 K. This leads to a small decrease in the slope of $\langle W^2\rangle_T$ and, consequently, to a flattening of the soft-phonon-frequency—squared curve. Simultaneously, a slight increase of the second-mode frequency occurs owing to the anticrossing effect between the two lowest branches. Thus large anharmonic coupling between the soft mode and the next TO mode enhances the deviation from the linear law in the curves of $\epsilon_0(T)$ or $\Omega_s^2(T)$. At infinite temperature, the core-shell constant becomes much larger so that the soft mode approaches the rigid-ion value, i.e., the saturation limit.

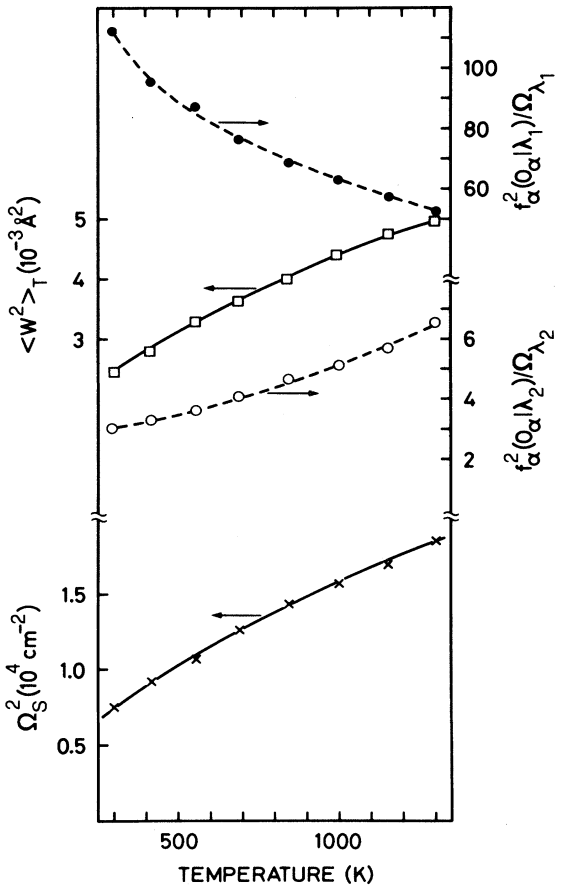

FIG. 12. Temperature dependence of the squared shell displacement $\langle W^2\rangle_T$ and of the soft-mode-frequency squared Ω_s^2. In the upper part, the $f_\alpha^2(O_\alpha\,|\,\lambda)/\Omega_\lambda$ contributions are represented for the two lowest-frequency modes at $q=0$. $\lambda_1=(q=0,\ j=1)$ denotes the soft mode and $\lambda_2=(q=0,\ j=2)$ the next-lower-lying TO mode [see Eq. (14)].

It should be noted that the model introduced by Migoni *et al.*[1] and used here in order to analyze the high-temperature saturation of the soft mode is, to our knowledge, in better agreement with the experimental data than other models.[49,50] In particular, the calculations of Cowley[49], which predicted the temperature dependence of TO and LO frequencies and their linewidths in $SrTiO_3$, yield an increase of *all* phonon frequencies with increasing temperature. This behavior is only verified for the two lowest-frequency TO modes and the intermediate LO mode, whereas a marked decrease of the three other modes is experimentally observed (see Fig. 7). As emphasized by Migoni *et al.*,[1] it seems that an unrealistic fourth-order anharmonicity parameter had been used in Ref. 49. If this parameter is modified, however, in order to account for the temperature dependence of the high-frequency modes, then the fourth-order anharmonicity alone becomes too weak to explain the saturation of the soft mode. The experimental data presented for $SrTiO_3$ in Ref. 13 and for $KTa_{0.982}Nb_{0.018}O_3$ in this work may more readily be interpreted in terms of the theory developed by Migoni *et al.*

VI. CONCLUSION

The deviation from the Curie-Weiss law and the saturation regime in the infinite-temperature limit—for the decoupled soft mode—evidenced in our experiments are understood in terms of a renormalization of the soft mode via an increase of the quartic anharmonic contribution in the electronic polarizability of the oxygen ion towards (Ta,Nb) ions.

In a previous work,[10] the nonlinear shell model developed by Migoni *et al.*[1] has been used to describe the low-temperature quantum ($T\ll 100$ K) and classical ($100<T<300$ K) regimes. With the present extension, it can be said that this model is applicable over the entire temperature range $0<T<1300$ K, and that it provides an explanation for the saturation effect at infinite tempera-

ture. It should be noted, however, that no change occurs in the dielectric response $\epsilon_0(T)$ [see Eq. (9)]: At very high temperatures (1000 K $< T$), $\gamma = 1$ still holds. This contradicts the prediction $\gamma = \frac{1}{3}$ obtained from a simplified pseudo-one-dimensional version[2] of the Migoni model where a coupling can only be taken into account between the soft mode and an acoustic mode.

In summary, the Migoni model provides a realistic picture of the temperature dependence of the soft mode in $KTa_{0.982}Nb_{0.018}O_3$ and accounts correctly for the saturation limit of this mode at infinite temperature.

ACKNOWLEDGMENTS

It is a pleasure to thank Claire-Lise Bandelier and Françoise Jenny for their help in the preparation of this work.

[1]R. Migoni, Ph.D. thesis, Max-Planck-Institut für Festkörperforschung, Stuttgart, 1975 (unpublished); R. Migoni, H. Bilz, and D. Bäuerle, Phys. Rev. Lett. 37, 1155 (1976); R. Migoni, H. Bilz, and D. Bäuerle, in *Proceedings of the International Conference on Lattice Dynamics,* edited by M. Balkanski (Flammarion, Paris, 1978), p. 650.

[2]H. Bilz, A. Bussmann, G. Benedek, H. Büttner, and D. Strauch, Ferroelectrics 25, 339 (1980); A. Bussmann-Holder, G. Benedek, H. Bilz, and B. Mokross, J. Phys. (Paris) Colloq. 42, C6-409 (1981).

[3]A. Bussmann-Holder, H. Bilz, D. Bäuerle, and D. Wagner, Z. Phys. B 41, 353 (1981).

[4]A. Bussmann-Holder, H. Bilz, and W. Kress, J. Phys. Soc. Jpn. 49, A737 (1980).

[5]A. Bussmann-Holder, H. Büttner, and H. Bilz, Ferroelectrics 35, 273 (1981).

[6]D. Bäuerle, D. Wagner, M. Wöhlecke, B. Dorner, and H. Kraxenberger, Z. Phys. B 38, 335 (1980).

[7]D. Wagner and D. Bäuerle, Phys. Lett. 83A, 347 (1981).

[8]M. D. Fontana, G. E. Kugel, and C. Carabatos, J. Phys. (Paris) Colloq. 42, C6-749 (1981).

[9]M. Löhnert, G. Kaindl, G. Wortmann, and D. Salomon, Phys. Rev. Lett. 47, 194 (1981).

[10]D. Rytz, U. T. Höchli, and H. Bilz, Phys. Rev. B 22, 359 (1980).

[11]Some preliminary results are given in D. Rytz, J. L. Servoin, and F. Gervais, Ferroelectrics 35, 817 (1981).

[12]M. Balkanski, M. K. Teng, M. Massot, and H. Bilz, Ferroelectrics 26, 737 (1980); M. Massot, M. K. Teng, J. F. Vittori, M. Balkanski, S. Ziolkiewicz, F. Gervais, and J. L. Servoin, *ibid.* 45, 237 (1982).

[13]J. L. Servoin, Y. Luspin, and F. Gervais, Phys. Rev. B 22, 5501 (1980).

[14]See, for example, S. K. Kurtz, Bell Syst. Tech. J. 45, 1209 (1966).

[15]S. Triebwasser, Phys. Rev. 114, 63 (1959).

[16]U. T. Höchli, H. E. Weibel, and L. A. Boatner, Phys. Rev. Lett. 39, 1158 (1977).

[17]U. T. Höchli and L. A. Boatner, Phys. Rev. B 20, 266 (1979).

[18]J. J. van der Klink, D. Rytz, F. Borsa, and U. T. Höchli, Phys. Rev. B 27, 89 (1983).

[19]R. C. Miller and W. G. Spitzer, Phys. Rev. 129, 94 (1963).

[20]C. H. Perry and T. F. McNelly, Phys. Rev. 154, 456 (1967).

[21]C. H. Perry and N. E. Tornberg, Phys. Rev. 183, 595 (1969).

[22]G. Shirane, R. Nathans, and V. J. Minkiewicz, Phys. Rev. 157, 396 (1967).

[23]W. B. Yelon, W. Cochran, G. Shirane, and A. Linz, Ferroelectrics 2, 261 (1971).

[24]P. A. Fleury and J. M. Worlock, Phys. Rev. Lett. 18, 665 (1967); Phys. Rev. 174, 613 (1968).

[25]H. Uwe and T. Sakudo, Phys. Rev. B 15, 337 (1977).

[26]S. K. Manlief and H. Y. Fan, Phys. Rev. B 5, 4046 (1972).

[27]Y. Yacoby and A. Linz, Phys. Rev. B 9, 2723 (1974).

[28]R. L. Prater, L. L. Chase, and L. A. Boatner, Phys. Rev. B 23, 221 (1981).

[29]W. G. Nilsen and J. G. Skinner, J. Chem. Phys. 47, 1413 (1967); C. H. Perry, J. H. Fertel, and T. F. McNelly, *ibid.* 47, 1619 (1967).

[30]F. Gervais and J. L. Servoin, in Reviews in Infrared and Millimeter Waves, edited by K. J. Button (Plenum, New York, in press).

[31]D. Rytz and H. J. Scheel, J. Cryst. Growth 59, 468 (1982).

[32]F. Gervais, in Electromagnetic Wave Phenomena in Matter, edited by K. J. Button (Academic, New York, in press).

[33]S. H. Wemple, Phys. Rev. 137, A2696 (1965); D. G. Demurov and Y. N. Venevtsev, Fiz. Tverd. Tela (Leningrad) 13, 669 (1971) [Sov. Phys.—Solid State 13, 553 (1971)]; W. R. Abel, Phys. Rev. B 4, 2696 (1971); G. A. Samara and B. Morosin, *ibid.* 8, 1256 (1973); R. P. Lowndes and A. Rastogi, J. Phys. C 6, 932 (1973); I. V. Ivanov, G. V. Belokopytov, I. M. Buzin, V. M. Sycher, and V. F. Chuprakov, Ferroelectrics 21, 405 (1978).

[34]G. Rupprecht and R. O. Bell, Phys. Rev. 135, A748 (1964).

[35]W. G. Spitzer, R. C. Miller, D. A. Kleinman, and L. E. Howarth, Phys. Rev. 126, 1710 (1962).

[36]A. S. Barker and J. J. Hopfield, Phys. Rev. 135, A1732 (1964).

[37]D. W. Berreman and F. C. Unterwald, Phys. Rev. 174, 791 (1968).

[38]Y. Luspin, J. L. Servoin, and F. Gervais, J. Phys. C 13, 3761 (1980).

[39]J. L. Servoin, F. Gervais, A. M. Quittet, and Y. Luspin, Phys. Rev. B 21, 2038 (1980).

[40]M. D. Fontana, G. Métrat, J. L. Servoin, and F. Gervais, Ferroelectrics 38, 797 (1981).

[41]F. Gervais, J. L. Servoin, J. F. Baumard, and F. Denoyer, Solid State Commun. 41, 345 (1982).

[42]J. F. Scott, Rev. Mod. Phys. 46, 83 (1974).

[43]F. Gervais and B. Piriou, J. Phys. C 7, 2374 (1974); Phys. Rev. B 10, 1642 (1974).

[44]F. Gervais and J. L. Servoin, Phys. Rev. B 15, 4532 (1977).

[45]J. L. Servoin and F. Gervais, Appl. Opt. 16, 2952 (1977).

[46]J. H. Barrett, Phys. Rev. 86, 118 (1952).

[47]K. A. Müller and H. Burkard, Phys. Rev. B 19, 3593 (1979).

[48]M. D. Fontana, G. E. Kugel, and C. Carabatos, in *Recent Developments in Condensed Matter Physics,* edited by J. T. Devreese, L. F. Lemmens, V. E. Van Doren, and J. Van Royen (Plenum, New York, 1980), p. 139.

[49]R. A. Cowley, Philos. Mag. 11, 673 (1965).

[50]A. S. Chaves, F. C. S. Barreto, and L. A. A. Ribeiro, Phys. Rev. Lett. 37, 618 (1976).